Electronic Supplementary Material (ESI) for Nanoscale.

Supporting Information

Fabrication of high aspect ratio nanogrid transparent electrodes *via* capillary assembly of Ag nanoparticles

Juhoon Kang[1,2], Chang-Goo Park[3,4], Su-Han Lee[3], Changsoon Cho[1,2], Dae-Geun Choi[3], and Jung-Yong Lee[1,2*]

[1]Graduate School of Energy, Environment, Water, and Sustainability (EEWS), [2]Graphene Research Center, Korea Advanced Institute of Science and Technology (KAIST), Daejeon 305-701, Republic of Korea, [3]Nano-Mechanical Systems Research Division, Korea Institute of Machinery & Materials (KIMM), Daejeon 305-343, Republic of Korea, [4]Department of Nano-Mechatronics, University of Science and Technology (UST), Daejeon 305-350, Republic of Korea

[*]All correspondence should be addressed to J.-Y.L. (email: jungyong.lee@kaist.ac.kr)

Size distribution of the AgNPs

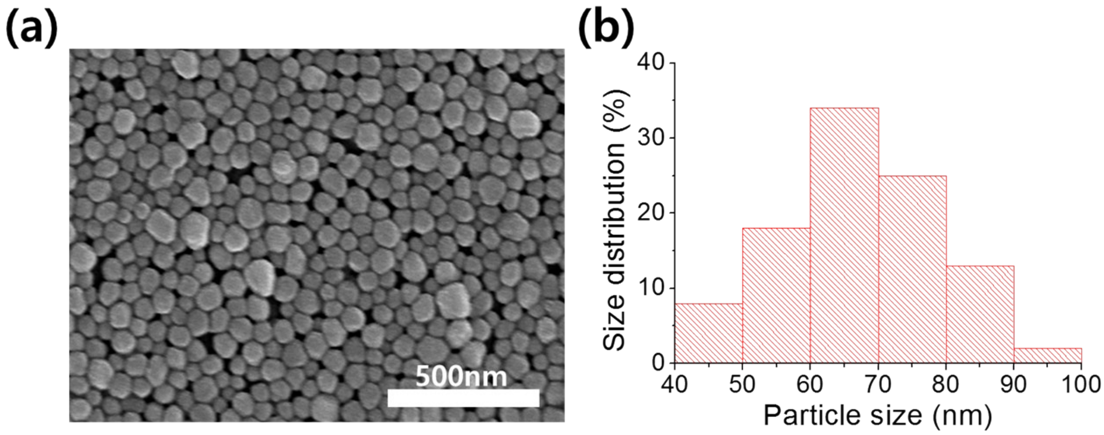

Figure S1. (a) The SEM images and (b) size distribution histogram of AgNPs.

Figure S1 shows SEM images and size distribution histogram of the synthesized AgNPs. Diameters of AgNPs are measured from SEM images. Average diameter of AgNPs obtained from 300 AgNPs is 66 nm.

Solvent injection rate

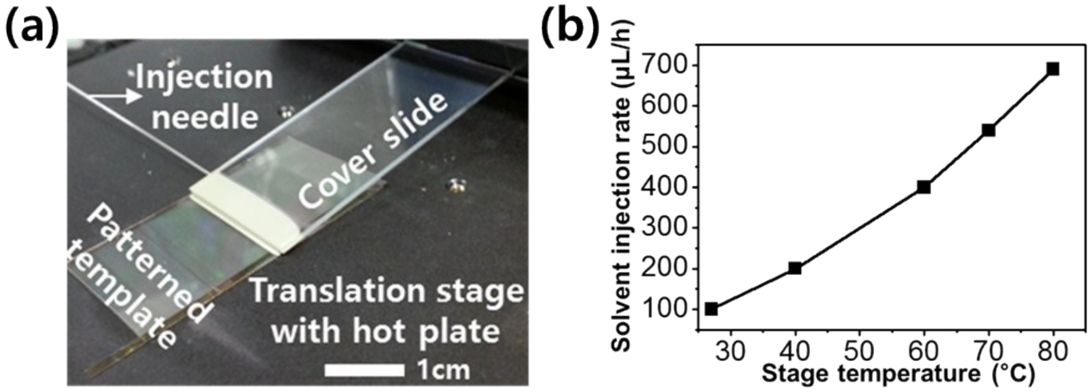

Figure S2. (a) Photograph of the capillary assembly setup. (b) Solvent injection rate according to the stage temperature

Water is continuously provided to the AgNP suspension during the capillary assembly process to maintain the contact angle of AgNP suspension. Figure S2(b) shows the solvent injection rate at a relative humidity of 30 ± 1 %.

Solvent injection during the fabrication process decrease the concentration of AgNPs because AgNPs in the suspension are deposited on the patterned nanogrid template while the volume of solvent remains almost unchanged. For 100 μL AgNP suspension (2 wt%), number of AgNPs in the suspension is approximately 1.27×10^{12}, which is estimated from the mass fraction (wt%) of AgNPs in the suspension, volume of individual AgNPs (spherical shape is assumed, average diameter = 66 nm) and density of silver (10.49 g/cm^3). Number of AgNPs deposited along the patterned nanogrid (1 $inch^2$ sample) is approximately $1.26 \times 10^{11}/inch^2$, which is estimated from the volume of individual AgNPs, the dimension of the nanogrid (150 nm × 450 nm × 3.2 μm), packing fraction (0.74, close-packing of sphere is assumed) and assembly yield (96 %). Therefore, after the fabrication of 1 $inch^2$ Ag nanogrid, estimated reduction of the AgNP concentration is approximately 9.9%.

Bubble formation at high stage temperatures

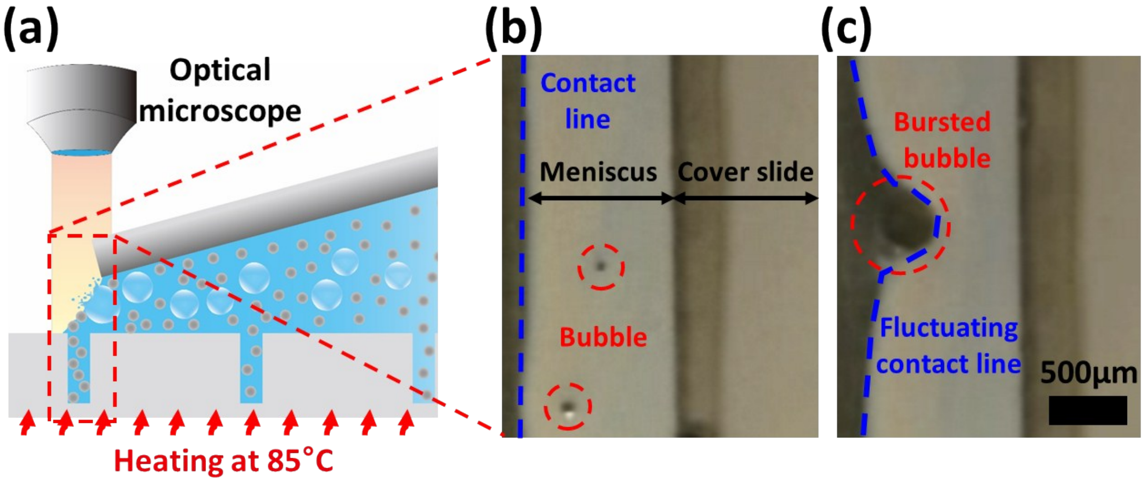

Figure S3. (a) Schematic illustration of bubble formation. Optical micrograph showing (b) bubbles at the meniscus and (b) fluctuating contact line

Bubble formation inside the AgNP suspension at a high temperature (> 85°C) makes the contact line fluctuate and disturbs the uniform capillary assembly of AgNPs. Bubbles formed inside the AgNP suspension move toward the meniscus of the AgNP suspension (Fig. S3(b)) and burst at the three phase contact line (Fig. S3(c)), leading to a fluctuating contact line.

Optimal fabrication speed at different AgNP concentration

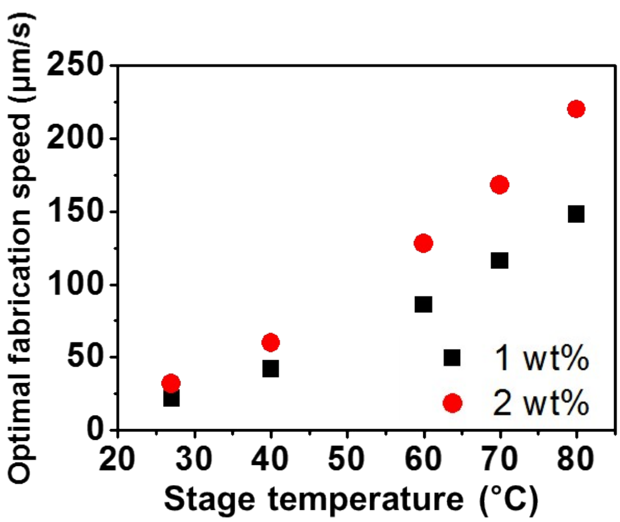

Figure S4. Optimal fabrication speed depending on the stage temperature and AgNP concentration

Figure S4 shows investigation of optimal fabrication speed depending on the stage temperature and AgNP concentration at the fixed relative humidity of 30 ± 1 %.

Transfer of residual AgNPs on the flat, top surface of a patterned template

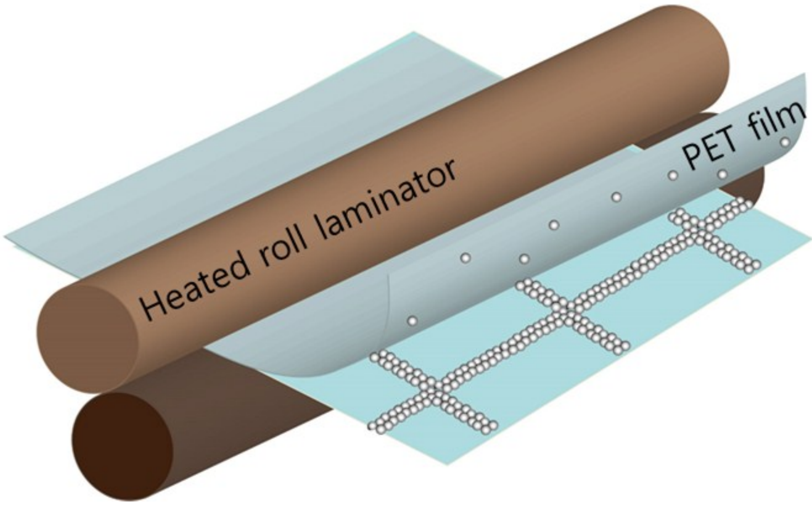

Figure S5. Transfer of residual AgNPs using a heated roll laminator

AgNPs deposited on the flat top surface of the nanogrid patterned template can be removed by transferring them onto the PET film using a heated roll laminator.

Thermal annealing of assembled AgNPs

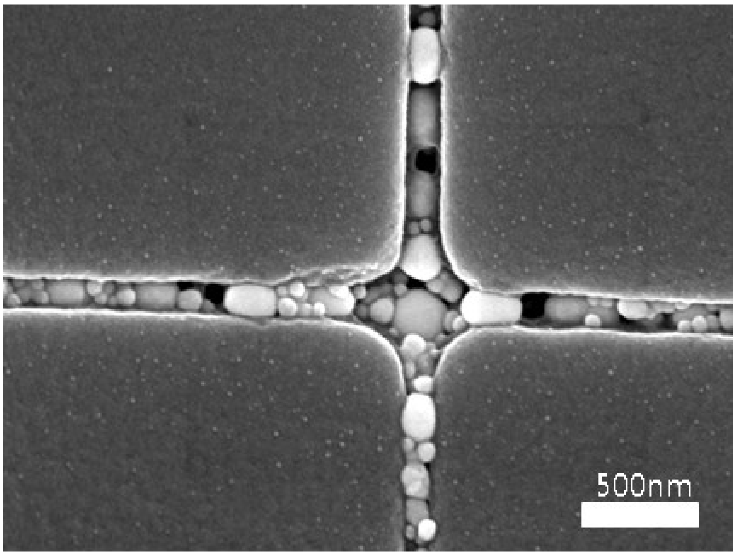

Figure S6. Agglomerated AgNPs after thermal annealing at 250 °C for 20 min

After thermal annealing of assembled AgNPs at 250 °C for 20 min, larger AgNPs are formed by the agglomeration of smaller AgNPs due to Ostwald ripening.

Morphological change of the Ag nanogrid by photochemical welding

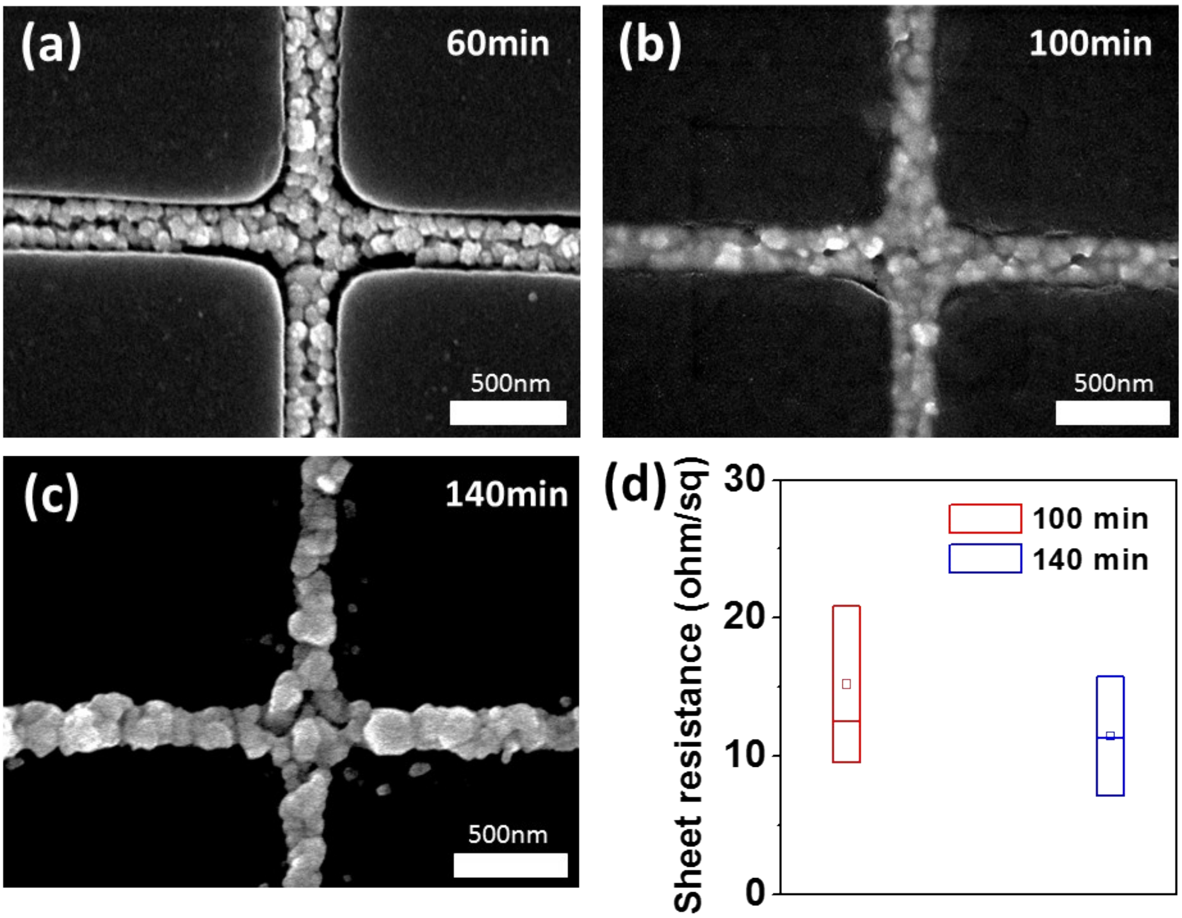

Figure S7. (a–c) Morphological changes of the Ag nanogrid with photochemical reaction time. (d) Sheet resistance of the Ag nanogrid after photochemical welding and post-annealing with respect to photochemical reaction time.

Figure S7 shows morphological change of the Ag nanogrid with photochemical reaction time. After 100 min of photochemical reaction and post-annealing, an average sheet resistance of 15.2 Ω/sq was obtained (Fig. S7(b)). Further photochemical reaction (140 min) led to a decrease in the sheet resistance to 11.4 Ω/sq. However, the Ag nanogrid grew over the flat surface of the nanogrid pattern and made the Ag nanogrid wider and rougher (Fig. S7(c)).